ISSN 0001-4370, Oceanology, 2022, Vol. 62, No. 3, pp. 404–420. © Pleiades Publishing, Inc., 2022.
Russian Text © The Author(s), 2022, published in Okeanologiya, 2022, Vol. 62, No. 3, pp. 466–484.

MARINE GEOLOGY

Evolution of Sedimentation Environment of Postglacial Basins in the Eastern Gulf of Finland during the Holocene under the Changing Climate

A. Yu. Sergeev[a, *], D. V. Ryabchuk[a], E. S. Nosevich[a], D. V. Prishchepenko[a], V. A. Zhamoida[a], A. L. Piskarev-Vasiliev[b, **], D. V. Elkina[b], L. D. Bashirova[c, *], E. P. Ponomarenko[c], L. M. Budanov[a], and A. G. Grigoriev[a]**

[a] *Karpinsky Russian Geological Research Institute (VSEGEI), St. Petersburg, Russia*

[b] *Gramberg All-Russia Scientific Research Institute for Geology and Mineral Resources of the Ocean (VNIIOKEANGEOLOGIA), St. Petersburg, Russia*

[c] *Shirshov Institute of Oceanology, Russian Academy of Sciences, Moscow, 117218 Russia*

**e-mail: sergeevau@yandex.ru*

***e-mail: apiskarev@googlemail.com*

****e-mail: bas_leila@mail.ru*

Received September 17, 2021; revised October 29, 2021; accepted December 16, 2021

Abstract—The paleoclimatic events of the Late Pleistocene and Holocene have been clarified based on the results of detailed lithological, geochemical, pollen, and paleomagnetic studies of sediment cores collected in the eastern Gulf of Finland. The time frame of the change from lacustrine to marine sedimentation conditions has been refined based on the radiocarbon dating. For deposits of the marine phase of the Baltic Sea in the eastern Gulf of Finland, hypoxia cycles associated with periods of warming during the Holocene have been revealed.

Keywords: pollen analysis, paleomagnetic properties, Ancylus Lake, Littorina Sea, Baltic Ice Lake, Holocene, Baltic Sea

DOI: 10.1134/S0001437022030122

INTRODUCTION

The Baltic Sea is one of the largest brackish inland seas (water surface area 419000 km^2) [21]. Its relatively shallow water depth (~50 m on average) and large catchment area (1641400 km^2) contribute to fairly high sedimentation rates (up to 1–6 m/ka) [35, 40]. Thus, Baltic Sea researchers have access to sediment archives that cover a relatively small geological time period (centuries to a first ten thousand years), but they are characterized by high resolution, which makes them an almost ideal object for analyzing changes in climate and natural conditions over the past 16 ka.

According to the current concept of the Baltic Sea evolution in the Holocene, there are several main stages: the Yoldia Sea (11.7–10.7 ka cal BP), the freshwater Ancylus Lake (10.7–9.8 ka cal BP), a transitional regressive phase identified in a number of publications as the Mastogloia Sea (9.8–8.5 ka cal BP), and the Littorina Sea, which formed ~8.5 ka cal BP as a result of the Baltic Basin final connection with the North Sea and Atlantic Ocean, as well as the Post-Littorina or modern phase (from 4.5 ka cal BP), when the sea level relatively stabilized and the coastal lines shape approached to the modern [24, 25].

The exceptional shallowness of the eastern Gulf of Finland, the relatively flat bottom and coastal topography, and the insignificant (from 0 to +2 mm/year) current glacioisostatic uplift rates have determined the existence and good preservation of late-postglacial landforms (including relict coastal formations) both above and below sea level [1, 46, 47].

In the frame of geological surveys carried out by VSEGEI in 1984–2000 in the eastern Gulf of Finland, deposits corresponding to different phases of the postglacial development of the Baltic Basin were identified mainly based on lithological features [22, 52] and the data of limited palynological, diatom, and palaeomagnetic studies [4, 7–9, 13, 18, 52, 53].

Modern high-resolution analytical methods and sediment core studies make it possible to resolve problems in reconstructing the parameters of the sedimentation and climate conditions [3, 5, 17, 29, 31–34, 38, 54, 57].

In the eastern Gulf of Finland, the first successful example of high-resolution sedimentological studies was an complex analysis of sediment core F40, performed as part of the international BONUS INFLOW project, which gathered data on changes in the sedimentary conditions over the past 6 ka and, in particular, new evidence on the timing of the Neva River break through to the Gulf of Finland (~3.3 ka cal BP) [19, 55].

In 2017–2020, VSEGEI specialists, funded by the Russian Science Foundation and Russian Foundation for Basic Research, commenced a cycle of sedimentological studies of bottom sediments in the eastern Gulf of Finland [48]. The objectives of this article is a complex detailed lithological and stratigraphic study of bottom sediments from the deepest sedimentary basin of the Russian part of the Gulf of Finland, located between the Gogland and Moshchny islands, in order to reconstruct the parameters of the sedimentation environment of paleo-waterbodies in the Holocene.

MATERIALS AND METHODS

Bottom sediment cores were recovered on cruise 35 of the R/V *Akademik Nikolai Strakhov* (2017), organized by the IO RAS and cruises aboard R/V *CH1303* (2017–2018), organized by VSEGEI. The study areas were selected based on results of analyzing the VSEGEI geological and geophysical databases compiled from geological shelf surveys (1980–2000). For targeted sediment core collection, sub-bottom profiling (SBP) was performed using a 3300-HM high-frequency profiler (EdgeTech, USA) with Discover Sub-Bottom v3.36 recording software and GEONT-SHELF HRP seismic station (Spektr-Geofizika, Russia). The article discusses the results of studies of three cores 177 to 482 cm long (Fig. 1). The cores were sampled in plastic pipes and transported to an onshore laboratory. To characterize the modern conditions at all stations, duplicate sampling of the undisturbed surface sediments was carried out using a box corer.

In the laboratory, the cores were sectioned, photographed, and described including the determination of colors according to the international Munsell Color Chart. For all cores, the distribution of chemical elements (Al, Si, P, S, Cl, K, Ca, Ti, V, Cr, Mn, Fe, As, Y, Zr, Ba and Pb) was studied by X-ray fluorescence analysis (OLYMPUS Innov-X XRF scanner).

For all cores, the grain size distribution was determined with a Microsizer 201A (VA Instal) laser particle analyzer. The sampling step for the analysis was 1 cm.

Geochemical studies (Sr, Pb, As, Zn, Cu, Ni, Co, Fe_2O_3, TiO_2, MnO, V, Cr, Br) were carried out with a SPECTROSCAN MAKC-G scanning X-ray analyzer with a step of 3 cm. Data on the distribution of Br concentrations along the vertical section of the core were used to calculate the paleosalinity of water basins [29].

180 samples were taken without gaps from the core 17GG-1t for pollen analysis. The laboratory workout was performed by Grichuk's extended method [6]. Sediments were placed at sodium pyrophosphate for disintegration and centrifuged in a heavy liquid. Microscope slides were prepared from the material washed of chemistry. The results were interpreted in accordance with [14–16, 42].

The radiocarbon dating of 14 sediment samples was performed at the Radiocarbon Dating and Electron Microscopy Laboratory of the Institute of Geography RAS and the Center for Applied Isotope Research of the University of Georgia (USA) performed using dispersed organic carbon (Table 1, Fig. 2). The IntCal20 calibration curve for terrestrial deposits and the CALIB 8.2 software were used for age calibration [43]. To verify the age model and calculate the "reservoir effect" we used the data on changes in the Pb content in bottom sediments of the 18MI-1t core over the last 2000 years, since the peaks in the Pb concentrations in Baltic Sea bottom sediments associated with the atmospheric deposition correspond to the exact calendar age of 750 ± 50 cal BP (1200 CE, medieval maximum) and the 1970s [44, 55, 59]. The calculated reservoir effect was +370 years [48], which agrees well with the earlier calculations for core F40 (+350 years) [55].

For all sediment cores, loss on ignition (LOI) and total organic carbon (TOC) were determined with 5 cm interval. In the Laboratory of Geology of Atlantic of IO RAS, TOC analysis was performed on an AN-7529M express carbon analyzer by automatic coulometric titration based on pH value according to the standard methodology [48].

The paleomagnetic studies were also carried out for two sediment cores, including natural remanent magnetization (NRM) measurements. Magnetic susceptibility was measured for all cores, and magnetic susceptibility anisotropy was measured with cubic samples in core17GG-1t.

The magnetic susceptibility of sediments was measured on the undisturbed surface of cores by a KT-5 kappameter and/or a Bartington MS2E sensor with 6.5 and 2.5 cm steps, respectively. During the MS2E measurements, the magnetic susceptibility values were corrected to eliminate equipment temperature drift. The magnetic susceptibility values were automatically recalculated by Multisus, Bartington software.

For core 17GG-1t, paleomagnetic measurements were performed using the equipment of the Center for Geo-Environmental Research and Modeling (GEOMODEL) of the Research Park in St. Petersburg State University. NRM measurements were performed on an SRM-755 SQUID magnetometer (2G Enterprises). After NRM measurements, to remove the viscous remanent magnetization induced by Earth's modern magnetic field, as well as to isolate other remanence components, including the most stable, the core was magnetically treated. Demagnetization with an alternating magnetic field was carried out with a step of 5 mT in the range of 5–30 mT and with a step

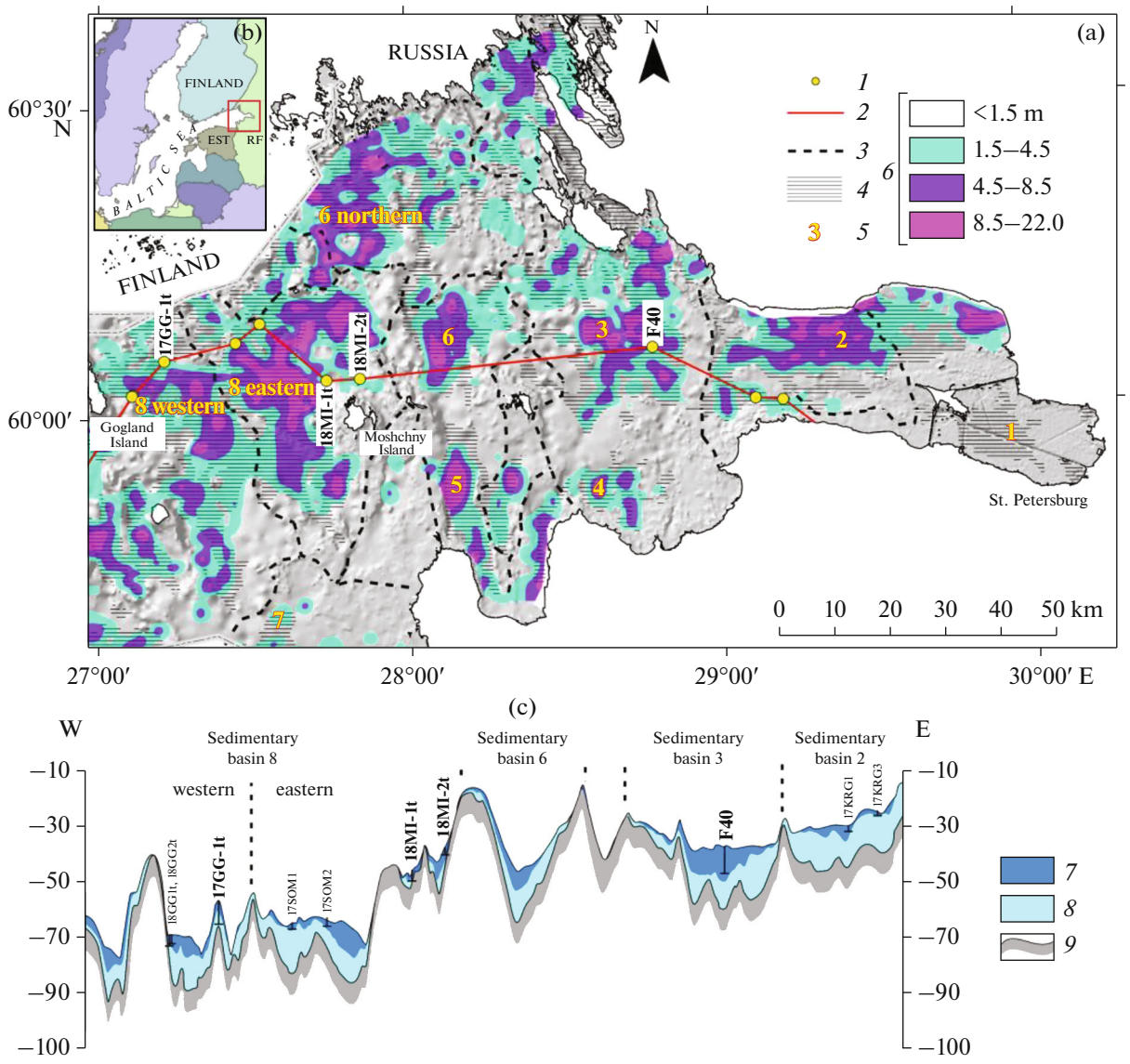

Fig. 1. Thickness diagram of Holocene sediments showing location of bottom sediment cores (a): (*1*) sediment core sampling sites; (*2*) line of geological section; (*3*) lines of convex inflection of bottom topography separating local sedimentary basins; (*4*) areas of modern sedimentation of silty clay bottom sediments; (*5*) number of local sedimentary basin; (*6*) thickness of Holocene sediments in meters according to SBP data. Position of study area on sketch map of Baltic Sea (b). Geological section showing location of bottom sediment cores (c): (*7*) marine and lacustrine Holocene sediments; (*8*) Late Pleistocene glacial–lacustrine deposits (massive and varved clays of Baltic Ice Lake); (*9*) surface of glacial deposits (moraine) of last glaciation.

of 10 mT starting at 30 mT, up to a maximum field of 100 mT. For the cubes from the upper 260 cm, magnetic susceptibility measurements were duplicated using an MFK1-FA Kappabridge.

Samples for paleomagnetic measurements in core 17GG-1t were taken continuously using plastic cubes with dimensions of 19 × 19 × 20 mm and an internal volume of ~8 cm^3. The cubes were pressed into intact sediment along the entire length of the core. Since the core was not oriented in the horizontal geographic plane during sampling, the cubes were oriented relative to the core coordinates for the *X* and *Y* components of the NRM vector, and in the vertical plane – downward along depth (*Z*). The size of the samplers determined the measurement resolution. After extraction, the cubes were cleaned of excess sediment and covered with a plastic lid, then stored in a refrigerator at an average temperature of +5°C. A total of 213 cubes were taken from core 17GG-1t (Fig. 2).

Based on the demagnetization results, principal component analysis (PCA) [37] was used to calculate the characteristic remanent magnetization (ChRM) component with the maximum angular deviation (MAD) in "Demagnetization Analysis in Excel" (DAIE) [49] mainly using demagnetization steps of 20–80 mT.

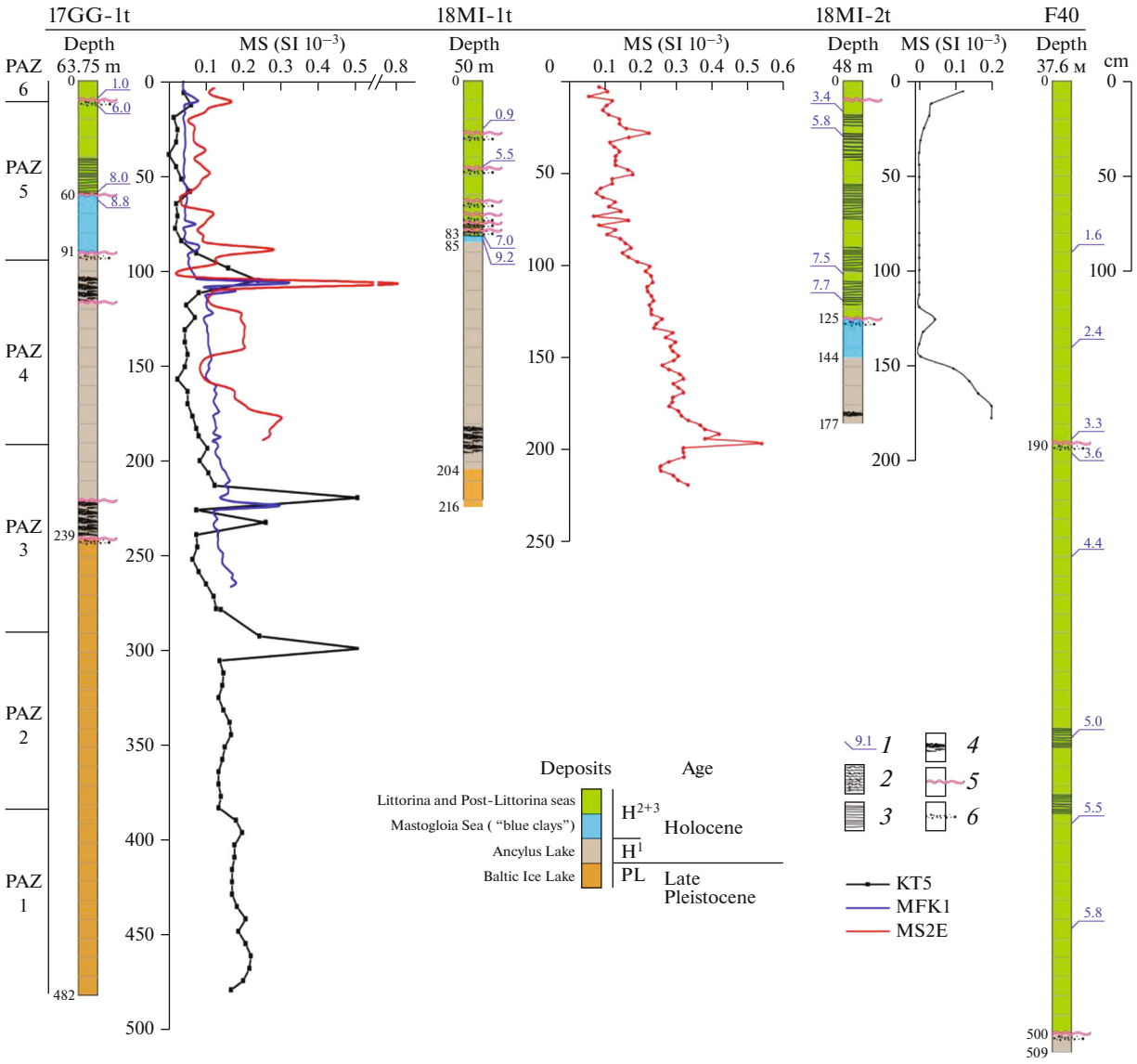

Fig. 2. Lithological and stratigraphic complexes of bottom sediment cores in eastern Gulf of Finland (core length in centimeters): (*1*) radiocarbon dating results (ka cal BP); (*2*) partially bioturbated deposits; (*3*) distinctly layered deposits; (*4*) interlayers of hydrotroilite (amorphous iron sulfide); (*5*) erosion boundaries; (*6*) enrichment in sandy material; PZ, palynozone and its number. Magnetic susceptibility curves obtained using different measurement methods: MFK1-FA, KT-5, MS2E.

RESULTS

Seismostratigraphy of bottom sediments. In the acoustic sections, six acoustic units (AU) are identified, the boundaries between which are delineated along continuous reflectors and/or significant changes in the recording infrastructure. AU-1 (moraine) on sections of high-frequency SBP is the acoustic basement. It has a high amplitude top boundary with a complex shape. The AU-1 is characterized by the absence or high attenuation of the reflection energy. AU-2 (varved clays) overlies AU-1 almost everywhere. The inner infrastructure of the record of records presented with series of sustained parallel in-phase reflections with relatively high-intensity. The layers of AU-2 are bedded consistent with the roof of the underlying unit. AU-3 is acoustically transparent and fills relative depressions in the roof of the underlying AU-1 and AU-2. When AU-3 developed above AU-2, sometimes a near-horizontal boundary can be distinguished within it. AU-4 (deposits of the Baltic Ice Lake) has an infrastructure similar to AU-2—on sections, it is represented by series of continuous parallel reflectors, but has a lower intensity of reflected signals. AU-5 (deposits of the Ancylus Lake) has a complex acoustic pattern—a series of near-horizontal reflectors with local zones of correlation loss (gaps in continuous boundaries). The complex is not ubiquitous and fills local depressions in the underlying (AU-4 or AU-2) units; the lower reflec-

Table 1. Results of radiocarbon dating of sediment cores

Laboratory Code $IGAN_{AMS}$	Core depth, cm	Dated material	^{14}C age ±1σ, BP	Calibrated age, cal BP, 1σ	Calibrated age, cal BP, 2σ	Calibrated age, cal BP, median	Calibrated age with reservoir effect
18MI-2t							
7975	16–17	Bulk sediment	3480 ± 20	3698–3824	3652–3831	3758	3388
7976	29–30	Bulk sediment	5370 ± 25	6034–6272	6008–6278	6190	5820
7977	100–101	Bulk sediment	6995 ± 30	7790–7919	7735–7931	7831	7461
7978	115–116	Bulk sediment	7315 ± 30	8040–8174	8031–8178	8105	7735
18MI-1t							
7561	24–25	Bulk sediment	1280 ± 20	1177–1271	1176–1277	1227	857
7562	44–45	Bulk sediment	5050 ± 20	5745–5891	5738–5896	5829	5459
7563	79–80	Bulk sediment	6505 ± 20	7340–7430	7330–7472	7379	7009
7564	83–84	Bulk sediment	8615 ± 25	9535–9592	9532–9676	9550	9180
7565	183–184	Bulk sediment	15540 ± 35	18803–18862	18770–18894	18833	18463
17GG-1t							
7160	9–10	Bulk sediment	1420 ± 20	1300–1343	1296–1347	1324	954
7161	12–13	Bulk sediment	5620 ± 20	6320–6440	6311–6449	6394	6024
7162	57–58	Bulk sediment	7540 ± 25	8348–8382	8223–8405	8366	7996
7163	60–61	Bulk sediment	8240 ± 25	9134–9276	9033–9399	9208	8838
7164	90–91	Bulk sediment	10620 ± 40	12623–12699	12498–12722	12658	12288

tors have a weakly expressed unconformity with the roof of the underlying deposits. AU-6 (deposits of the Littorina and Post-Littorina Sea) completes the section and is slightly more widespread than AU-5. The unit is exposed as a series of near-horizontal continuous reflections of varying intensity, usually more intensive than in AU-5. The deposits of the complex contain gas-saturated sediments, which are characterized by a zone of chaotic reflections with almost complete attenuation of acoustic signal below it.

Lithology and geochemistry of bottom sediments. *Core 17GG-1t* was sampled in the western part of the sedimentary basin at a depth of 63.75 m (Figs. 1–3). The core has length of 482 cm and covers deposits of AU-4–AU-6.

Lower interval (482–239 cm) is represented by homogenous or banded massive clays. Color banding consists of interlayered thin (fractions of mm) layers of gray and brown colors (10YR6/2, 5YR5/6, 5YR6/4, 5YR5/2, 10YR6/2). The grain size distribution reveals two intervals: the sediments of the lower (482–300 cm) are characterized by a finer composition — the average content of the clay fraction[1] is 80.9%; silt — 13.4%; sand — 5.7%); sediments of the upper (300–239 cm) contain 76.6% clay, 18.1% silt, and 5.4% sand particles.

The geochemical parameters vary insignificantly along the section and have a distribution similar to variations in the grain size composition of the deposits. The peak of Zr content is recorded at core depth of 300 cm.

The distribution of the calculated paleosalinity along the core section in 482–239 cm interval has a uniformly sawtooth pattern, ranging from 0 to 2‰ (Fig. 4). The distribution of the bulk of the studied chemical elements correlates to the clay fraction distribution.

The 239–95 cm interval consists of grayish brown clays and silty clays (5X6/1). An important diagnostic feature of the deposits are black "sooty" nodules up to 1–2 mm in diameter (N1 black). Weakly magnetic nodules, which are a mixture of several mineral phases—pyrite, melnikovite, and partially oxidized hydrotroilite [48], cause sharp peaks on the magnetic susceptibility curve (Fig. 2). The nodules are concentrated in individual pockets up to 1 cm in diameter and, sometimes, into lenticular layers. The most distinct layer is confined to the 239–223 cm interval. It is interesting to note that fluctuations in K, Si, and Cu contents are observed within the hydrotroilite horizons, but Fe content does not change. In the 239–95 cm interval, the grain size composition of sediments differs from the underlying sediments. Layers enriched in larger fractions stand out. These are silty clays in the 239–227, 224–223, and 222–217 cm intervals, where the content of fraction is 53.5–69.6% (average 64.4%); silty clays—24.0–41.4% (average 31.0%); sandy—3.3–6.4% (average 4.6%). In the interval 239–170 cm, there is a gradual increase in the content of clay particles (from 64 to 82%); the opposite trend is a decrease in the content of clay particles from 82 to 62% in the of 170–91 cm interval.

Si, K, and Zr contents are more variable than in the underlying interval. The calculated paleosalinity (1.1–1.5‰) remains low, except for the upper 20 cm where it increases to 2.5–3‰ (Fig. 4).

The upper contact at the 95 cm level is marked by an interval of clayey silt enriched in sand particles (content of clay particles — 38.7%; silt particles — 42.0%; sand particles — 19.3%). The thickness of the interval is 1 cm. The described contact is characterized by a peak of Zr content, which is associated with an increase in the terrigenous component and a relative increase in the amount of sand particles. Most of the distribution curves of the geochemical indicators are characterized by kinks, which indicate a rather sharp change in the sedimentation conditions. A radiocarbon dating of 12.3 ka cal BP was obtained for the top of the layer (Table 1).

Further up-core, there is an interval of "blue clays" of 34 cm thick (60–95 cm interval), which is sharply distinguished by lithology. The grain size distribution mode of the deposits shifts towards silt fractions, the grain size distribution is fairly consistent within the interval: sediments are represented by bluish gray (5G6/2) clayey silt and silty clay (the content of particles is 40.4–63.1% (average 49.2%); silt—32.0–55.9% (average 46.5%); sand—2.7–9.0% (average 4.3%)). In the 60–70 and 88–91 cm intervals, spots of finely dispersed organic matter (OM) are noted; in the 71–80 cm interval, horizontal layering (banding) is observed due to enrichment in OM. In the blue clays, a sharp increase in Mn content is recorded; the value of the calculated paleosalinity increases abruptly from 2 to 7‰. The interval has been dated to 8.8 ka cal BP (60–61 cm) (Table 1). Due to the low thickness, the interval is not identified on acoustic profiles (Fig. 3).

The section of core 17GG-1t is crowned by deposits corresponding to AU-6. The thickness of these deposits is significantly reduced comparing to central part of the described sedimentary basin, where it exceeds 2 m and in other sedimentary basins–5 m (station F40, 14-T3, etc. [48]). In core 17GG-1t, the deposits are subdivided into three layers based on lithological features. The lower layer (60–31 cm) is represented by greenish gray (5Y4/1) layered clayey silts; the middle layer (31–11 cm) is represented by bioturbated clayey silts without pronounced bedding. The upper layer (0–11 cm) consists of soft brownish unstratified silty clay. The grain size distribution of sediments changes abruptly at the base of the complex compared to the underlying "blue clays." The silt frac-

[1] Here and below, we use the granulometric classification of L.B. Ruhina <0.005 mm—pelite, 0.005–0.05 mm—silt, 0.05–2 mm—sand.

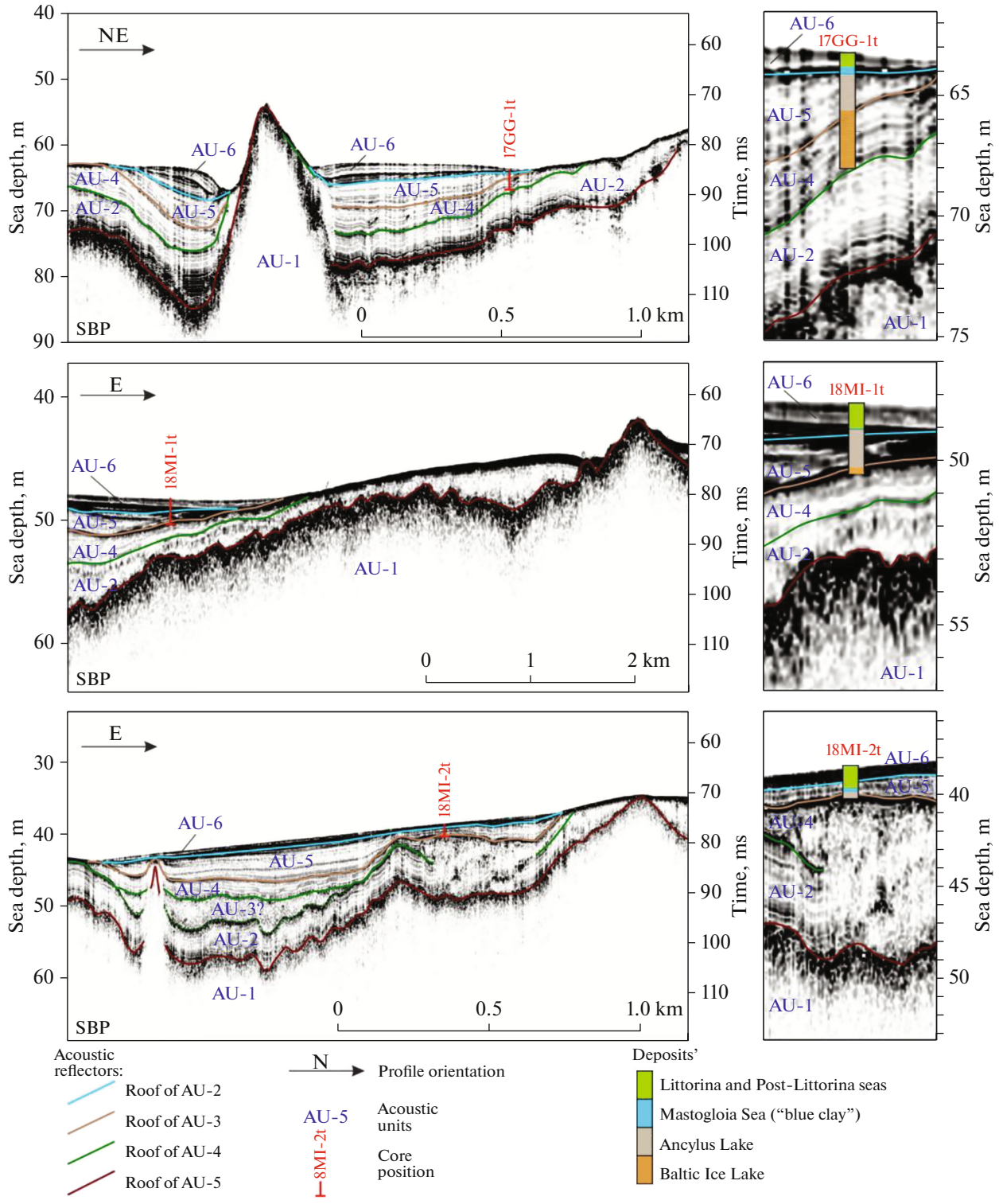

Fig. 3. Position of cores 17GG-1t, 18MI-1t, 18MI-2t on SBP profiles.

tion becomes dominant (the content of silt particles is 47.4–65.1% (average 58.4%)), the share of the clay fraction decreases to 31.1–49.2% (average 39.2%), and the sand admixture is still insignificant (2.6–8.0%, average 3.4%). The lower (erosive) contact is emphasized by peak TiO_2, K, and Zr concentrations. Upwards, an increase in paleosalinity (up to 9.6‰) is noted. Two dates have been obtained for these deposits: 57–58 cm — 8.0 ka cal BP; 12–13 cm — 6.0 ka cal BP (Table 1, Fig. 4).

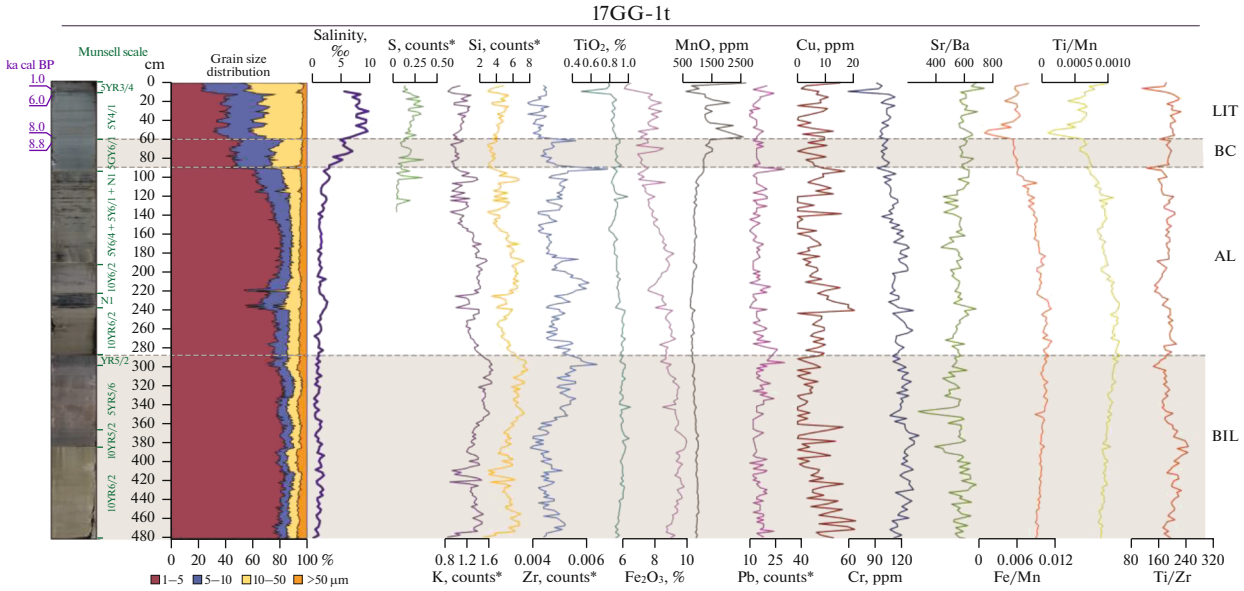

Fig. 4. Photo of core, grain size and some geochemical parameters of core 17GG-1t. Deposits: BIL, Baltic Ice Lake; AL, Ancylus Lake; BC, blue clay of Mastogloia Sea; LIT, Littorina Sea.

In the 14–11 cm interval, there is an abrupt change in the grain size distribution of sediments. The erosion horizon is characterized by a sharp change in Zr, K, TiO_2, and Si contents as well as an abrupt decrease in the calculated paleosalinity. The share of the clay fraction decreases to 22.2–26.1% (average 23.7%), the content of the sand fraction is 1.9–6.7% (average 3.8%), and the maximum content of sand particles is noted at the lower boundary of the interval. Up-core, in 0–11 cm interval, there is an interval of brownish gray (5YR3/4) soft silty clays, in which a trend towards a gradual increase in the content of relatively coarser fractions is expressed. For the 9–10 cm horizon, a dating of 1.0 ka cal BP was obtained (Table 1, Fig. 4).

Cores 18MI-1t and *18MI-2t* were sampled in the eastern part of the sedimentary basin (Fig. 1) at depths of 48 and 38.25 m, respectively. In 218–204 cm interval, core 18MI-1t reached AU-4 deposits, represented by grayish brown (5X6/1) silty clays and clays (the content of clay fraction varies from 68 to 79.6%, 73.0% on average) with pronounced color banding. In the 204–85 cm interval, deposits are gradually replaced by brownish gray silty clays (content of clay fraction — 51.1–77.7%, average 66.8%) (AU-5). Within the 196–187 and 133–108 cm intervals, sediments are sharply enriched in lenses, nodules, and spots of sooty color. Both the grain size distribution and content of chemical elements vary insignificantly along the interval (Fig. 5a). For the 183–184 cm horizon of core 18MI-1t, a dating of 18.5 ka cal BP was obtained (Table 1). Core 18MI-2t exposed only the upper part of AU-5 (177–144 cm interval) (Fig. 5b). Sediments are represented by brownish gray (5X6/1) silty clays; an interval of hydrotroilite was recorded at a core depth of 174–171 cm. The mean LOI and TOC values in both cores are 4.8 and 0.6%, respectively, and there is a slight increasing trend in these indicators upwards the interval.

The upper boundary of the AU-5 deposits in both cores is marked by a sharp change in grain size distribution and an abrupt increase in LOI and TOC (up to 6.0 and 1.0%, respectively).

A “blue clay” layer (5G6/2) is recorded in both cores: a thin one (2 cm) in the 85–83 cm interval of core 18MI-1t and more pronounced (19 cm) in the 144–125 cm interval of core 18MI-2t. Sediments are represented by silty clays (content of clay fraction — 56.5–69%, average 62.8%). In core 18MI-1t, starting from this layer and further up-core, an increase in the calculated paleosalinity is observed; a sharp enrichment in sandy material (up to 45.2%) is recorded at the upper contact of the layer. Core 18MI-1t is dated to 9.2 ka cal BP at 83–84 cm (Table 1, Fig. 5a).

Further up-section in core 18MI-1t, the “blue clay” layer is replaced by greenish gray (5G6/1) bioturbated (83–30 cm) and greenish gray laminated (30–0 cm) clayey silts. The grain size parameters are characterized by significant variability (the content of the clay fraction varies from 24.7 to 54.8%, average 37.1%). There are six erosion horizons with an increased content of sand particles (up to 11% at 80–81 cm; 9.3% at 77–78 cm; 9.3% at 75–76 cm; 8.4% at 66–67 cm; 16.1% at 47–48 cm; and 18.0% at 29–30 cm). In these layers, an increased content of Zr is recorded (Fig. 5a). Following radiocarbon dates were obtained for the core: above the lower contact of the 79–80 cm layer — 7.0 ka cal BP; above the two upper erosion horizons — 5.5 ka cal BP at 44–45 cm and 0.9 ka cal BP at 24–25 cm (Table 1).

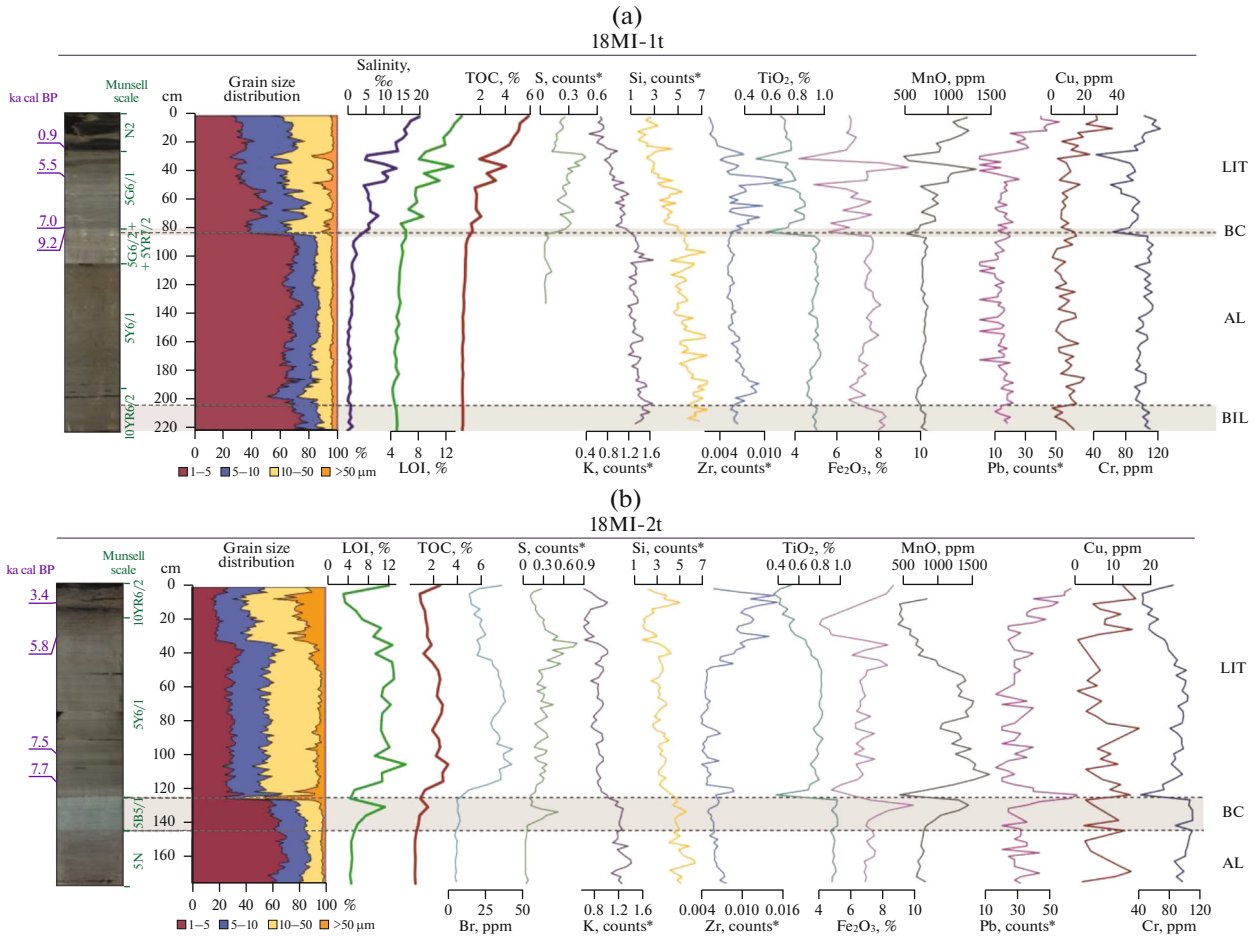

Fig. 5. Photos of cores, grain size and some geochemical parameters: (a) core 18-MI-1t, (b) core 18-MI-2t. Deposits: BIL, Baltic Ice Lake; AL, Ancylus Lake; BC, blue clay of Mastogloia Sea; LIT, Littorina Sea.

In core 18MI-2t, erosion horizons enriched in sand, except for the 6–8 cm interval, are not expressed. However, three intervals are distinguished according to changes in the grain size distribution, geochemistry, and textural features of the deposits (Fig. 5b). The average content of the clay fraction is 30.5% in the 125–33 cm interval, 19.2% in the 33–6 cm interval, and 24.2% in the 6–0 cm interval. The lower interval begins with 10 cm-thick layer of greenish gray bioturbated clayey silt; further up-core until 33 cm depth, there is alteration of horizontally laminated and non-laminated bioturbated greenish gray clayey silts. Lamination disappears above 68 cm. A weak regressive trend is noted in the grain size distribution, and enrichment in sand (up to 37%) is recorded at the upper boundary of the interval. In the upper intervals, an increase in TOC is observed, along with change in calculated salinity from 1.6 to 20‰. The geochemical parameters are consistent along the section and change sharply in the 33–6 cm interval (Fig. 5b). The 6–0 cm interval is represented by black non-laminated clayey silts. The following dates are obtained for the core deposits: 7.7 ka cal BP (115–116 cm), 7.5 ka cal BP (100–101 cm), 5.8 ka cal BP (29–30 cm), and 3.4 ka cal BP (16–17 cm).

Palynological analysis. Based on the results of pollen analysis of core 17GG-1t, six pollen assemblage zones (PAZ) were identified (Fig. 6).

PAZ 1 (485–380 cm) is characterized by a relatively low pollen content. Trees predominate (from 72.0 to 83.9%), *Pinus* (up to 29.5%), *Betula* (up to 49.7%), and *Betula nana* (up to 12.9%). *Picea* makes up to 13.5%. *Quercus* and *Corylus* grains are found in the upper part of the zone; *Salix* presents widely, but does not exceed 1.6%. Herbs (up to 26.4%) are presented by Ericaceae (up to 7.7%), Poaceae (up to 7.5%); Asteraceae (up to 2.4%) and *Artemisia* (up to 2.3%) have been mentioned. Spores are presented by Polypodiaceae and *Lycopodium*; in the lower part of the zone *Sphagnum* has been noted; at the upper part *Equisetum* was found. A large number of algae cysts were recorded, and single testate amoebas were found in the lower and middle parts of the palynozone.

In PAZ 2 (380–288 cm) *Pinus* increases (up to 33.6%). *Betula* dominates (up to 34.2%); *Betula nana* average content is 5.5% with maximum 20.0% in the

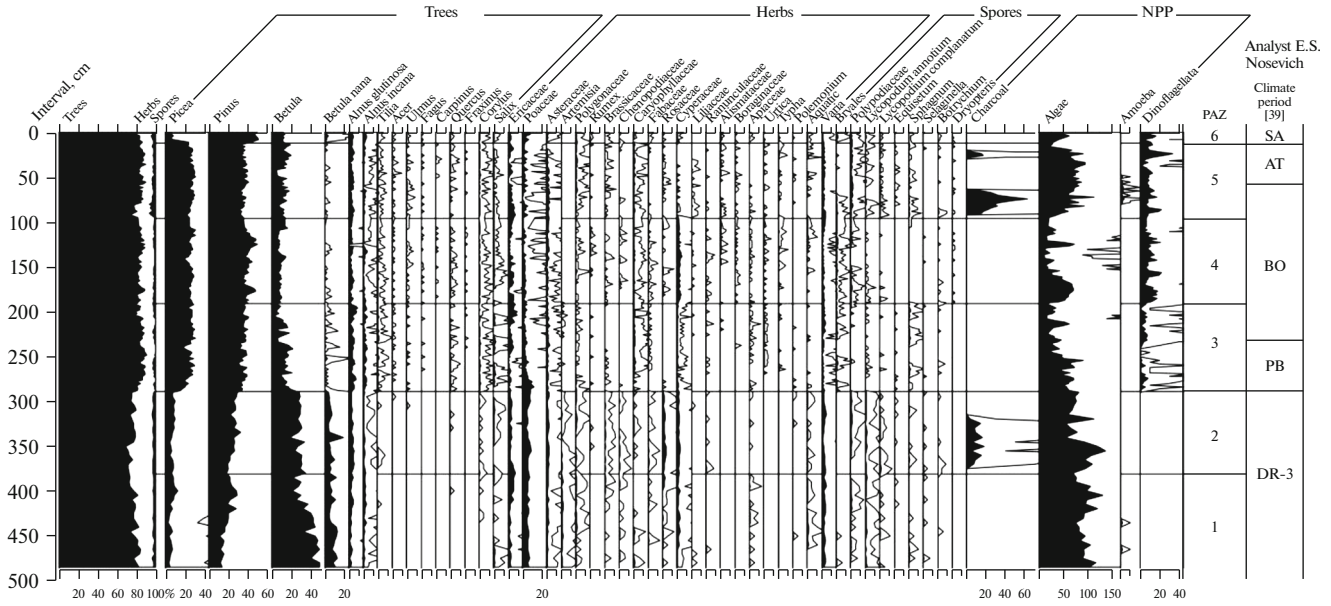

Fig. 6. Pollen diagram of core 17GG-1t sediments (compiled by E.S. Nosevich); climatic period is given after [39].

lower part of the zone. *Tilia, Acer, Quercus* and *Ulmus* present throughout the entire zone; *Corylus* reaches 1.0%. *Picea* maximum makes up 10.2%. Trees do not exceed 81.9%. Herbs reaches 27.0%. Poaceae present up to 11.7% in the upper part of the zone, Ericaceae (up to 4.4%) are distinguished. Rosaceae and Cyperaceae are mentioned (3.4% each), as well as *Artemisia* (up to 1.2%). Polypodiaceae, *Lycopodium*, and *Selaginella* have been recorded throughout the zone. A large number of charcoal particles was noted.

In pollen spectra of PAZ 3 (288–190 cm) *Picea* (up to 31.4%) and *Pinus* (up to 41.7%) increases, *Betula* (up to 18.3%) and *Betula nana* diminishes (up to 1.8%). Broadleaves species, including *Fagus*, are found throughout the zone and count up to 2.6%. *Salix* reaches 2.3%. Thus, trees makes up to 90.4%. Herbs (up to 19.5%) are dominated by Ericaceae (up to 9.5% in the upper part of the zone), Poaceae (up to 10.2% in the lower part); *Urtica* and *Typha* have been noted in the upper part of the zone. *Artemisia* has been mentioned, but then its grains disappear from the spectra. Spores are few: Bryales and *Sphagnum* have been identified. Dinoflagellate cysts appear in samples.

PAZ 4 (190–95 cm) characterizes by a high pollen concentration. Trees dominate (up to 88.7%), *Pinus* (from 34.7 to 51.1%) and *Picea* (from 19.9 to 31.6%) are mostly spread, as well as *Betula* (up to 16.5%). *Fagus, Ulmus,* and *Fraxinus* have been noted, as well as *Carpinus* throughout the zone. Herbs (up to 18.9%) present, Cyperaceae (up to 5.3%), Ericaceae (up to 6.1%), and Poaceae (up to 3.6%) are distinguished. Apiaceae and Fabaceae are mentioned. Bryales, Polypodiaceae, *Botrychium*, singly *Dryopteris* have been recorded. Cysts of dinoflagellates and algae were found.

In PAZ 5 (95–11 cm) the highest pollen concentration throughout the core was noted. Trees make up to 89.9%. *Picea* (up to 31.3%), *Pinus* (up to 44.2%), and *Betula* (20.4%) dominate. *Fagus, Carpinus* and *Fraxinus* are found. Herbs (up to 22.4%) are presented by Poaceae (up to 5.4%), Ericaceae (up to 7.8%), and Asteraceae (up to 3.5%), as well as Polygonaceae (up to 2.0%) and Caryophyllaceae (up to 2.2%). Liliaceae, Alismataceae, and *Typha* are mentioned in the lower part of the zone. Bryales spores are noted; *Sphagnum, Equisetum, Selaginella*, as well as *Dryopteris* present. Charcoal, algae cysts and single valves of testate amoebae were found closer to the lower part of the zone.

In PAZ 6 (11–0 cm) trees dominate (up to 83.9%), *Pinus* (up to 51.3%). *Picea* (up to 8.4%), *Betula* (up to 13.1%), *Betula nana* (up to 4.4%) are present; broadleaves are abundant (up to 2.6% in total). Herbs (up to 17.2%) are represented by Poaceae (up to 7.9%), Ericaceae (up to 3.4%), and Asteraceae (up to 1.3%). Anthropogenic *Rumex, Urtica*, Cereales and Alismataceae have been recorded. Bryales, Polypodiaceae, and *Botrychium* have been noted.

Paleomagnetic research. Figure 7 shows the results of paleomagnetic measurements of core 17GG-1t. The bulk of demagnetized samples show very low MAD values (<5), which indicates the high reliability of the obtained ChRM inclinations and declinations, as well as the presence of one main component that bears the magnetization, not counting the viscous one. An exception is samples of the first meter, the NRM of which is initially quite low, reflected in the demagnetization results as a certain range of magnetization within values close to those of the holder for magnetometer under high alternating fields. Together with

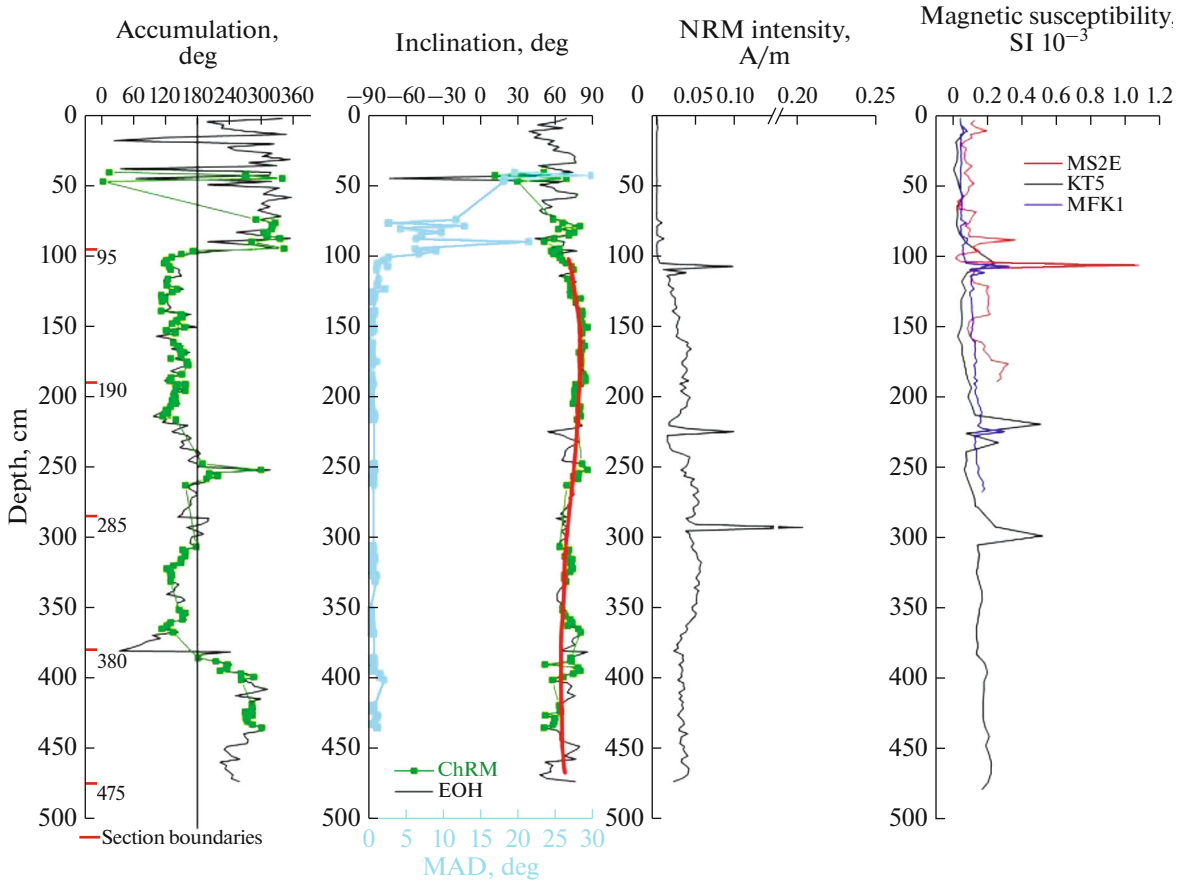

Fig. 7. Paleomagnetic parameters of core 17GG-1t. Inclination and declination of characteristic remanent magnetization (ChRM) are shown in green; NRM curve and declination, inclination, and intensity of NRM curves are shown in black. Light blue curve, maximum angular deviation (MAD). Magnetic susceptibility curves obtained using different kappameters: dark blue, MFK1; red, MS2E; black, KT-5. In 460–100 cm interval, red curve shows trend of change in inclination value.

the low magnetic susceptibility, this reflects the relatively low content of magnetic minerals in Littorina deposits.

The radiocarbon dating was performed for Littorina Sea sediments in the upper part of the core. It was determined that the interval from 60 to 14 cm below the sea bottom has age of 8.0–6.0 ka cal BP. Within these deposits, secular variations in the direction of the NRM vector are visible despite the fluctuations in the calculated parameters associated with low NRM values and, as a result, high MAD values. Another reason for the large fluctuations in the NRM in the Littorina deposits is that such distribution is characteristic for Northern European sedimentary sequences with age of 4.5–7.5 ka cal BP during the Solovki excursion, the maximum development of which took place 6 ka cal BP [2]. Earlier, based on a study of lacustrine sediments in Great Britain [26–28] and Fennoscandia [50], reliable data were obtained on significant changes in this declination and inclination time interval.

According to the data shown in Fig. 7, as well as the magnetic susceptibility curves of cores 18MI-1t and 18MI-2t (Fig. 2), the change in the regime of sedimentation between the Littorina and Ancylus complexes was accompanied by a significant change in the magnetic and paleomagnetic properties of the sediments. Ancylus deposits have a higher magnetic susceptibility and NRM. This allows high-accuracy determination of declination and inclination in this interval of the section, which is reflected by low MAD values. Deposits at a depth greater than 100 cm are characterized by small disordered declination fluctuations and regular changes in inclination. The general variability of the inclination curve in this interval fits into a half-cycle with an amplitude of change in inclination of ~15°, with values from 62° to 77°. According to the [26–28, 50], published data the characteristic total period of fluctuations in inclination for the age interval of 33–6 ka cal BP is 3–4 ka.

DISCUSSION

During deglaciation of the bottom of the Gulf of Finland, near the edge of a glacier, periglacial lakes formed, the area of which increased until the forma-

tion of a single Baltic Ice Lake, the level of which significantly exceeded the modern one. In the eastern Gulf of Finland, this period corresponds to a sedimentary complex that is clearly distinguished on the SBP profiles due to the layered structure and surrounding bedding, beginning with laminated clays, in which the layers thickness gradually decreases from 10–20 cm to fractions of a millimeter,—and massive nonlayered clays with color banding [48, 52]. The radiocarbon dating of these deposits is problematic due to the low organic content. In some cases, the upper contact of lacustrine–glacial deposits can be determined by the presence of erosion horizon enriched in silty-sandy material, since the final phase of evolution of the Baltic Ice Lake was marked by a "catastrophic paleogeographic" event: drainage of water into the ocean, when the level of the water dropped sharply by 25–27 m [24], which further continued to decline over several hundred years. However, the presence of such layer in bottom sediment cores is not found ubiquitous; in some cases, the change in lithology and grain size distribution of sediments occurs gradually.

Due to the impossibility of radiocarbon dating of lacustrine–glacial deposits, the results of paleomagnetic and palynological studies of core 17GG-1t are of particular interest.

Based on visual description, the upper contact of the deposits of the Baltic Ice Lake could be inferred at the 239 cm interval, above which an interlayer of grayish brown clays enriched in hydrotroilite is distinguished. However, the absence in the paleomagnetic record of an interval lithologically corresponding to the deposits of the Baltic Ice Lake, as well as data on the Gothenburg excursion, which is ~13 ka cal BP, makes it possible to limit the formation time of these deposits to a later age, and according to these data, the Holocene boundary (11.7 ka cal BP) is located approximately at a depth of 300–295 cm. The general variability of the inclination curve in the range of 460–100 cm in core 17GG-1t fits into a half-cycle with an amplitude of change in inclination of ~15°. Consequently, the probable duration of sedimentation in this interval is ~2 ka. This is confirmed by palynological studies, the results of which indicate a sharp change in vegetation, corresponding to the beginning of the Holocene at a core depth of 288 cm (Fig. 6). In the 482–288 cm interval, two palynozones were identified, which indicate cold and humid climatic conditions. The presence of cold-tolerant species and the relatively low participation of conifers in the structure of the vegetation cover allow us to date this stage of formation of catchment vegetation to the Baltic Ice Lake. Thus, according to palynological analysis and paleomagnetic data, the boundary of the beginning of the Holocene in the core did not coincide with the visually recognizable changes in the lithology of the deposits, and the boundary is located 20–30 cm below the lower contact of the hydrotroilite horizon.

The deposits of AU-5 are interpreted as sediments of Ancylus Lake. The variations of the grain size distribution within this unit, along with the "Pre-Ancylus" regression of the basin, in some cases demonstrate similar trends: a decrease in the median particle size in the lower part of the interval and increase towards the upper boundary of the unit. Earlier [48], we hypothesized that such a change in grain size distribution indicates transgressive–regressive cycles in the Early Holocene. In general, the grain size parameters and the curves of their changes, as well as the distribution of chemical elements and their ratios indicate basin sedimentation in relatively deep-water conditions. Geochemical parameters in core 17-GG-1t indicate accumulation of AU-5 deposits during gradual regression of the basin (Fe/Mn, Ti/Mn) and a decrease in the transport distance of sedimentary material (Ti/Zr) (Fig. 5). An exception is the content of chemical elements within hydrotroilite horizons, where the distribution of most chemical elements and their ratios are more variable. The sedimentation rates are at least 1.6 mm/year. The calculated paleosalinity (2–3‰) indicates the freshwater character of the paleo-basin.

According to existing ideas for the region of the eastern Gulf of Finland based primarily on paleolimnological and geoarchaeological studies on land [45, 47], the final stage in the evolution of Ancylus Lake was of regressive nature. At this stage, the first intrusion of saltwater into the Baltic Sea basin took place. The data of pollen analysis performed for core 17GG-1t indicate significant warming (PAZ 4) at the end of this stage. In this case, the nature of the change in grain size distribution can also be explained by increased land runoff associated with humidization of the climate.

The transitional horizon from lacustrine to marine deposits traced in cores 17GG-1t, 18MI-1t, and 18MI-2t is the most interesting and informative from the paleogeographic viewpoint. In all the studied cores, a lithologically specific "blue clay" layer with a thickness of 3 to 30 cm was revealed, characterized by a sharp change in grain size distribution (the grain size distribution mode shifts towards silt fractions) and geochemical parameters. At the lower boundary of the layer, there is also an increase in OM content (LOI up to 8.4%, TOC up to 1.2%), S, Mn, Br, and calculated paleosalinity (from 2 to 6–7‰). In the "blue clay," lithological and geochemical relationships change significantly with respect to the underlying deposits: the behavior of almost all the considered elements is indifferent with respect to the grain size distribution. These deposits were dated for the first time in cores 17GG-1t and 18MI-1t to 8.8 and 9.2 ka BP, respectively.

The "blue clay" layer was described for the first time in [36] and most fully analyzed in [56]. In the eastern Gulf of Finland, the "blue clay" layer was mapped during sampling in a frame of geological survey of the shelf at a scale of 1 : 200000 (VSEGEI, 1984–2000).

Only in the eastern most part of the Russian sector of the Gulf of Finland, adjacent to the Neva Bay, the "blue clay" horizon is absent in bottom sediment cores. In most cores where the upper parts of the section of Ancylus deposits were sampled, the thickness of the "blue clay," judging by the visual description, ranged from 1 to 10 cm. Up to the present, only two sediment cores have been studied, 09-BI-3 and 17-G-30-2, sampled in the Russian part of the Gulf of Finland and containing a "blue clay" layer with a thickness of 8 and 6 cm, respectively. In both cores, the lower and upper contacts are sharp, erosive, and enriched in sandy material [20].

The data agree well with the ideas on the paleogeographic evolution of the Baltic Sea. According to published data [24], this period corresponded to a decrease in the level of the basin and the first weak inflows of salt water into the Western Baltic and the Bornholm Basin [23, 25], dated to 9.8 ka cal BP. The period of 9.8–8.5 ka cal BP has been dated by different authors as the initial stage of the Littorina transgression (Initial Littorina Sea) [23] or Mastogloia Sea [3].

A sharp change in the sedimentation conditions influenced by the marine transgression at a low initial level of the basin led to transformation of the lithological and geochemical characteristics of the deposits. According to A.I. Blazhchishin [3], in the Arkona Basin (central Baltic), in some places in the upper (regressive) part of the "Ancylus-Lake Holocene" section sediment, layer enriched in allochthonous organic detritus is observed. In the section of sediments sampled on an underwater terrace at a depth of 45 m south of the Kriegers Flak Bank (southern Baltic), the Ancylus regression maximum corresponds to a peat layer that was formed under subaerial conditions. At the contact of the Ancylus and Littorina deposits in the Western Baltic, layer (5–15 cm thick) of gray sand containing plant detritus and a complex of diatoms from the Mastogloia Sea is widespread [3]. Above this horizon, sandy sapropel occurs in the Arkona Basin, and humic silt 10–30 cm thick occurs in Mecklenburg Bay (Southwestern Baltic). The formation of these deposits is associated with further regression of the Mastogloia Sea, and the described deposits correlate with the formation of the lower horizon of thinly layered sapropels, which in shallow areas are replaced by peaty interlayers [3]. In the Gdansk Deep, this time interval corresponds to layer represented by olive-gray silty clays with rare 1- to 5-mm-thick lenticular dark bands and black micronodules [29]. I. Harff [32] in the Gotland and Bornholm basins identified deposits of the initial phase of the Littorina transgression as an independent horizon (B1), characterized by distinct layering (banding) preserved in the section, which formed under reducing conditions with a lack of oxygen at the bottom–water boundary.

In the northern Baltic Sea, the Gulf of Bothnia, and Gulf of Finland, these transitional deposits are represented by the "blue clay" layer. In reference cores of the Northern Baltic Sea (MGML and AS2 stations [48]), these deposits of 46 cm-thick, overlying typical Ancylus silty clays with layers of hydrotroilite, are subdivided into two intervals (with a gradual transition), — bottom to top: gray clays with patchy enrichment with finely dispersed organic matter (32 cm) and bluish gray clays (14 cm). The diagnostic feature of this complex of deposits is the appearance of numerous diagenetic well-crystallized sulfides, which formed as pseudomorphs inside the benthic-fauna [56]. The greatest enrichment in sulfides is recorded, as a rule, in a thin interlayer. Identification of pyrite is confirmed by X-ray diffraction phase analysis [10]. The pyrite content, which makes up the entire heavy fraction, in "blue clays" can reach 0.1–0.3% (wt % of sediments). Micronodules can be represented by several varieties: (1) single black and bronze-yellow globules (up to 0.05 mm in size) and their xenomorphic intergrowths (up to 0.5–0.65 mm in size); (2) massive isometric golden nodules (up to 0.5–0.6 mm); (3) branching dendritic formations up to 2–50 mm long and with a cross-sectional diameter of a millimeter, which are pyrite biomorphoses along the borrowing paths of benthic fauna [11, 12]. Thus, it is important to note that the lithologically specific deposits of the transitional lacustrine–marine stage of the Baltic Sea were formed in the study area under conditions exceptionally favorable for the development of the benthic fauna. The lower contact of these deposits is either emphasized by a sandy layer (e.g., in core 17GG-1t, the >2.0 mm fraction increases to 45%), or it is characterized by an increased content of silt particles (e.g., in core 18MI-2t). A significant sedimentation hiatus, marked by an erosional horizon the base of the Littorina deposits, was also previously identified by the authors during a study of core F40 [19, 55].

The deposits of the lithological–stratigraphic complex crowning the geological section are characterized by the maximum variability of grain size and geochemical parameters, as well as the TOC content, which reflects multiple changes in the sedimentation conditions of the marine sedimentary basin. In the studied cores of Littorina deposits, one to four erosional horizons were revealed, as well as a number of intervals in which a sharp change in lithological and geochemical characteristics occurs. The Littorina deposits noticeably differ in color and texture from the underlying deposits; in all cores, the TOC content in them sharply increases, as well as the calculated salinity, which is associated with an increase in primary production, or with better OM preservation under hypoxic conditions [24, 51, 58].

In a number of publications based on sedimentological studies of the cores obtained from the Central and Southeastern Baltic [32, 57], core correlation schemes have been proposed based on alternating lithogeochemical parameters and textural features of deposits associated to climate change.

The dating of the Littorina section, performed for the first time for sediments of the eastern Gulf of Finland, made it possible to compare these results with data from other areas of the Baltic Sea. Dating of the deposits immediately above the contact with "blue clay" of 8.0 and 7.0 ka cal BP in cores 17GG-1t and 18MI-2t, respectively, show that typical sediments of the marine basin began to form in the sedimentary basin near Gogland Island almost simultaneously with the deposits of the initial phase of the marine transgression established in the Central Baltic. In most studies, the radiocarbon dating of the onset of the transgression lies between 8.5 and 8 ka BP [23, 51].

The first phase of development of the Littorina Sea in the central Baltic (B1 [32]) has been dated at 8.1–6.0 ka cal BP and is characterized as transitional from brackish to marine conditions with dominant anoxic conditions in the bottom water layers, which contributed to the preservation of thin lamination in the section undisturbed by benthic activity. This time interval corresponds to the lower layers of Littorina deposits in cores 17GG-1t and 18MI-2t, dated to 8–6 and 7.7–5.8 cal BP, respectively. At the base of the interval of these cores, just like in the previously studied cores of the same sedimentary basin [48], horizontally thin-laminated deposits are distinguished, which are indicators of an anoxic environment. In core 18MI-2t, the upper boundary of these laminated deposits is dated 7.5 ka cal BP. The thickness of the laminated bed in core 17GG-1t is similar, which suggests that anoxic conditions existed in this sedimentary basin from the onset of the Littorina transgression to its maximum phase (dated from data of studies of lakes on the Karelian Isthmus [41] at 7.3 ka cal BP). On the graphs of geochemical parameters, this interval is characterized by an increased Br content; in core 18MI-2t a trend towards a decrease in Ti content is observed, and in core 17GG-1t, a change in the ratios of chemical elements (Fe/Mn, Ti/Mn), which are indicators of decreased supply of material from land and deepening of the basin [32]. In cores 17GG-1t and 18MI-1t, sediments that formed between 7.0 and 6.0 ka cal BP are characterized by non-laminated structure or by the presence of individual groups of layers with a dominant massive sediment structure (core 18MI-2t) and light color, indicating the presence of oxygen in the bottom environment. A similar pattern was established for sediments cores in the Central Baltic based on research data [57], according to which this time period was characterized by cooling in the Baltic region, replaced by sharp warming at ~6 ka cal BP (according to an earlier publication [32], the date of this change in sedimentation conditions was determined as 5.7 ka cal BP), which again led to prevailing anoxic conditions in the bottom environment and formation of layered sediments. In core 17GG-1t, deposits above the interval with an age of 6 ka cal BP are crosscut by a thick erosion horizon, followed by a long sedimentation hiatus, which resumed only 1 ka cal BP.

In core 18MI-1t, deposits of the initial phase of the Littorina transgression were not preserved in the section. Dating of the lower layer of Littorina deposits in core 18MI-1t showed an age of 7.0 ka cal BP. This layer is characterized by a relatively coarser grain size composition compared to the overlying deposits and includes four peaks of enrichment in sandy material, which indicates a rather active hydrodynamic situation in the bottom layer during the formation of these deposits and the presence of sedimentation hiatuses.

In the cores recovered in the Northern Baltic [30], there are also laminated sediments under hypoxic/anoxic conditions in the bottom waters, caused by increased stratification of the water column during the early phase of the Littorina transgression as well as by an increase in OM input into bottom sediments. Increased productivity of surface waters is explained by an increase in temperature during the initial phase of the Holocene Thermal Maximum, as well as by regeneration of phosphorus from bottom sediments. The 47–28 cm interval in core 18MI-1t is represented by laminated, greenish gray silty clays; element-by-element distribution curves show an increase in the S and Mn contents. The calculated salinity increases to 14‰ at a depth of 37 cm. As mentioned above, such conditions have been established for the Central Baltic from 6.0 ka [57].

A close age of the formation of laminated Littorina deposits (5.5 ka cal BP) was obtained earlier for core F40, located in the central part of the sedimentary basin east of core 18MI-1t. In the previously studied core F40 [19, 55], the described deposits directly overlie the surface of the Ancylus clays (above the erosion horizon). Thus, the sedimentation hiatus during the initial phase of the Littorina transgression in the central part of the sedimentary basin south of the Berezovye Islands (sedimentary basin 3) was even longer.

CONCLUSIONS

Detailed sedimentological studies of bottom sediments in the westernmost sedimentary basin of the Russian part of the Gulf of Finland (between Gogland and Moshchny islands) made it possible to reconstruct the paleoclimatic conditions of postglacial waterbodies, date the main phases of their evolution, and reveal regional features of sedimentation processes.

(1) Sedimentation in the Baltic Ice Lake took place under the cold and humid climatic conditions, in a fresh waterbody characterized by low nutrient levels. The transition from lacustrine–glacial to lacustrine sedimentation was characterized by complete restructuring of sedimentation processes; in seismic sections, this transition is fixed by a stratigraphic unconformity, a change in the nature of bedding, and the transition to "focal" accumulation in limited sedimentary basins. In the section, the transition from Baltic Ice Lake to Ancylus sediments is usually accompanied by erosion

horizons enriched in sandy material and a sharp change in the spore–pollen spectra. In some cases, based on palynological analysis and paleomagnetic data, the position of the boundary of the beginning of the Holocene in the core does not coincide with the visually determined change in lithological composition (lower contact of the hydrotroilite horizon), but is 20–30 cm lower, which is also reflected in the change in grain size distribution of the deposits.

(2) The sediments of Ancylus Lake were formed in a fresh waterbody under conditions of climate warming and increased runoff from land. The final stage of existence of the waterbody had a regressive nature.

(3) The short-term regressive phase of the Mastogloia Sea in the region of the Gulf of Finland has been dated at ~9 ka cal BP and was expressed in the formation of a lithologically specific blue clay interlayer under conditions of an abrupt increase in salinity and bioproductivity of the waterbody.

(4) For deposits of the marine phase of evolution of the Baltic in the eastern Gulf of Finland, hypoxia cycles associated with warming periods have been identified. The onset of marine sedimentation in the sedimentary basin near Gogland has been dated at 8.0 ka cal BP. Sediments of the first phase of the Littorina transgression (8.0–7.0 ka cal BP) formed under anoxic conditions in the bottom environment. The period between 7.0 and 6.0 ka cal BP was characterized by the dominance of an oxygen-rich environment at the bottom–water boundary, which contributed to active development of benthos. The climatic conditions of the Early Holocene reconstructed for core 17GG-1t were milder than at present for at least part of the sea catchment area, and the salinity exceeded the modern level. In general, the bioproductivity of the Littorina Sea significantly exceeded the bioproductivity of the paleowaterbodies of the lacustrine–glacial and lacustrine stages of the Baltic Sea.

(5) A characteristic feature of the eastern Gulf of Finland is the recurring sharp change in sedimentation conditions in the Middle–Late Holocene and the presence of long sedimentation hiatuses due to regressions and erosion horizons formed during a relative decrease in sea level.

(6) The change in the nature of sedimentation between the Littorina and Ancylus complexes was accompanied by a significant change in the magnetic and paleomagnetic properties of sediments. The Ancylus deposits have a markedly higher magnetic susceptibility and NRM. The probable duration of sedimentation in the 460–100 cm interval in core 17GG-1t is ~2 ka, and the probable sedimentation time is 13–10 ka cal BP.

FUNDING

Studies of bottom sediment cores and processing of geophysical data were supported by the Russian Science Foundation (grant no. 17-77-20041-P). paleomagnetic studies supported by the Russian Foundation for Basic Research (project no. 19-05-00768). Acoustic profiling was carried out within the state assignment of IO RAS (topic no. FMWE-2021-0012).

REFERENCES

1. A. V. Amantov, V. A. Zhamoida, D. V. Ryabchuk, et al., "Geophysical structure of underwater terraces of the eastern part of the Gulf of Finland and simulation of the conditions for the formation at post-glacial stage of the development of the region," Regional'naya Geol. Metallogeniya No. 50, 15–27 (2012).
2. V.G. Bakhmutov and D. V. Glavatskii, "Problems of magnetostratigraphy of the Pleistocene loess and soil sediments of the south of Ukraine," Geofiz. Zhur. **38**, 59–74 (2016).
3. A. I. Blazhchishin, *Paleogeography and Evolution of Late Quaternary Buildup of Sediments in the Baltic Sea* (Yantarnyi Skaz, Kaliningrad, 1998) [in Russian].
4. V. P. Butylin, V. A. Zhamoida, M. B. Kozin, et al., *Lithostratigraphy of Upper Quaternary Sediments of the Gulf of Finland and Their Correlation with Similar Structures of the Central Baltic Region* in *Geology of Subaquatic Zone of the Joint of the Baltic Shield and Russian Platform within the Gulf of Finland* (VSEGEI, Leningrad, 1989) pp. 32–51. [in Russian].
5. A. G. Grigoriev, V. A. Zhamoida, M. A. Spiridonov, et al., "New data on the history of development of the south-eastern part of the Baltic Sea from the late postglacial period to nowadays," Regional'naya Geol. Metallogeniya No. 40, 103–114 (2009).
6. V. P. Grichuk and M. Kh. Monoszon, *Manual for Identification of single-stranded spores of the fern of* Polypodiaceae R. Br. *Family Growing in the USSR. Methodical Guide for Analysis of Spores and Pollen* (Nauka, Moscow, 1971).
7. R. N. Dzhinoridze, N. A. Gei, and A. E. Rybalko, "On the paleogeography of the Gulf of Finland in late Holocene," Vestnik St. Petersburg Gos. Univ., Ser. 7. No. 4 82–88 (1994).
8. R. N. Dzhinoridze and G. I. Kleimenova, "Materials for paleobotanical characteristic of late- and postglacial sediments of the Lakhta depression," Dokl. AN SSSR **161**, 700–703 (1963).
9. R. N. Dzhinoridze and G. I. Kleimenova, "Materials for paleobotanical Characteristic of Late- and Postglacial Sediments of the Lakhta Depression," in *Problems of paleogeography* (Leningrad Gos. Univ., Leningrad, 1965), pp. 193–214 [in Russian].
10. T. V. Dominikovskaya and V. A. Zhamoida, "Mineralogical Features of the Upper Quaternary Sediments in the Gulf of Finland," in *Glacial Shelves: Problems of Geology and Methodology of Study* (VSEGEI, Leningrad, 1985), pp. 35–43 [in Russian].
11. V. A. Zhamoida, Lithology and mineralogical features of the Upper Quaternary deposits of the glacial shelf Candidate's/Doctoral Dissertation in Geology and Mineralogy (VSEGEI, Leningrad, 1987).
12. V. A. Zhamoida, "Comparative Aspects of the Authigenic Formation of Minerals in Quaternary Sediments

of the Glacial Shelf Seas and Use of Authigenic Minerals for Stratification of Transverse Sections", in *Residual Mantle of the Glacial Shelf of North-Western Seas of Russia* (St. Petersburg, 1992), pp. 97–104 [in Russian].

13. V. V. Kochegura and B. Sh. Rusinov, "Paleomagnetic Differentiation and Correlation of Pleistocene and Holocene Sediments of the Gulf of Onega," in *Interdisciplinary Marine Geological and Geophysical Surveys of the Inner Seas of Glacial Shelves* (Leningrad, 1987), pp. 63–71 [in Russian].
14. L. A. Kupriyanova and L. A. Aleshina, *Pollen of Dicotyledon Plants of the Flora of the European Part of the USSR* (Nauka, Leningrad, 1978) [in Russian].
15. L. A. Kupriyanova and L. A. Aleshina, *Pollen and Spores of the Plants of the Flora of the European Part of the USSR* (Nauka, Leningrad, 1972) [in Russian].
16. L. A. Kupriyanova and L. A. Aleshina, *Spores of Pteridosperms and Pollen of Gymnospermous and Monocotyledonous Plants of the Flora of the European Part of the USSR* (Nauka, Leningrad, 1978) [in Russian].
17. *Litho- and Biostratigraphy of Seabed Sediments of the Baltic Sea*, Ed. by V. K. Gudelis (Vilnius, 1985) [in Russian].
18. D. B. Malakhovskii, Kh. A. Arslanov, N. A. Gei, et al., "New Data on the Holocene History of the of Lake Ladoga," in *Evolution of Natural Conditions and the Current State of the Lake Ladoga Geosystem* (Izd. Ross. Geograf. Obshch., St. Petersburg, 1993), pp. 61–73 [in Russian].
19. D. V. Ryabchuk, A. G. Grigoriev, V. A. Zhamoida, et al., "New data on the Formation of the Neva River based on the results of sedimentological studies in the eastern part of the Gulf of Finland," Regional'naya Geol. Metallogeniya, **61**, 6–20 (2015).
20. D. V. Ryabchuk, A. G. Grigoriev, T. V. Sapelko, et al., "Characteristic of the sediment processes in late glacial water bodies based on studies of the columns of seabed sediments in the eastern part of the Gulf of Finland," Ross. Geograf. Obshch., **149**, 32–52 (2017).
21. *Baltic Sea System* (Nauchnyi Mir, Moscow, 2017) [in Russian].
22. M. A. Spiridonov, "Glacial History of the Gulf of Finland," in *Geology of Subaquatic Zone of the Joint of the Baltic Shield and Russian Platform within the Gulf of Finland* (VSEGEI, Leningrad, 1989), pp. 15–23 [in Russian].
23. E. Andren, T. Andren, and G. Sohleniu, "The Holocene history of the southwestern Baltic Sea as reflected in a sediment core from the Bornholm basin," Boreas **29**, 233–250 (2000).
24. T. Andren, S. Bjorck, E. Andren, et al., "The Development of the Baltic Sea Basin During the Last 130 Ka,"in *The Baltic Sea Basin*, Ed, by J. Harff, S. Bjorck, and P. Hoth (Springer, Berlin, 2011).
25. B. E. Berglund, P. Sandgren, L. Barnekow, et al., "Early Holocene history of the Baltic sea, as reflected in coastal sediments in Blekinge, southeastern Sweden," Quat. Intern. **130**, 111–139 (2005).
26. K. M. Creer and P. Tucholka, "On the current state of lake sediment paleomagnetic research," Geophys. J. R. Astr. Soc. **74**, 223–238 (1983).
27. K. M. Creer, "Review of lake sediment paleomagnetic surveys," **7**, 125–160 (1985).
28. K. M. Creer and P. Tucholka, "Secular variation as recorder in lake sediments: a discussion of North American and European results," Philos. Trans. R. Soc. Lond. A **306**, 87–102 (1982).
29. A. Grigoriev, V. Zhamoida, M. Spiridonov, et al., "Late-Glacial and Holocene paleoenvironments in the Baltic Sea based on a sedimentary record from the Gdansk Basin," Climate Research **48**, 13–21 (2011).
30. K. Hausler, M. Moros, L. Wacker, et al., "Mid to late holocene environmental separation of the northern and central Baltic Sea basins in response to differential land uplift," Boreas **46**, 111–128 (2017).
31. J. Harff, G. Bohling, J. Davis, et al., "Physicochemical stratigraphy of Gotland basin Holocene sediments, the Baltic Sea," Baltica **14**, 58–66 (2001).
32. J. Harff, R. Endler, E. Emelyanov, et al., "Late Quaternary Climate Variations Reflected in Baltic Sea Sediments," in *The Baltic Sea Basin*, Ed. by J. Harff, S. Bjorck, and P. Hoth (Springer, Berlin 2011).
33. J. Harff, R. Lampe, and W. Lemke, et al. "The Baltic Sea – a model ocean to study interrelations of geosphere, ecosphere and anthroposphere in the coastal zone," J. Coastal Res. **21**, 441–446 (2005).
34. O. Hyttinen, N.Quintana Krupinski, O. Bennike, et al., "Deglaciation dynamics of the Fennoscandian ice sheet in the Kattegat, the gateway between the North Sea and the Baltic Sea basin," Boreas **50**, 351–368 (2021).
35. H. Ignatius, "On the rate of sedimentation in the Baltic Sea," Bull. Comm. Geol. Finland **180**, 135–145 (1958).
36. H. Ignatius, E. Kukkonen, and B. Winterhalter, "Notes on a pyritic zone in Upper Ancylus sediments from the Bothnian Sea," Bull. Geol. Soc. Finland **40**, 131–134 (1968).
37. J. L. Kirschvink, "The least-squares line and plane and the analysis of paleomagnetic data," Geophys. J. Int. **62**, 699–718 (1980).
38. A. T. Kotilainen, L. Arppe, S. Dobosz, et al., "Echoes from the past: a healthy Baltic Sea requires more effort," AMBIO **43**, 60–68 (2014).
39. J. Mangerud, S. T. Andersen, B. E. Berglund, and J. J. Donner, "Quaternary stratigraphy of Norden, a proposal for terminology and classification," Boreas **3**, 109–128 (1974).
40. J. Mattila, H. Kankaanpaa, and E. Ilus, "Estimation of recent sediment accumulation rates in the Baltic Sea using artificial radionuclides ^{137}Cs and $^{239,\,240}$Pu as time markers," Boreal Environment Res. **11**, 95–107 (2006).
41. A. Miettinen, L. Savelieva, D. A. Subetto, et al., " paleoenvironment of the Karelian Isthmus, the easternmost part of the Gulf of Finland, During the Litorina Sea stage of the Baltic Sea history," Boreas **36**, 441–458 (2007).
42. P. D. Moore, J. A. Webb, and M. E. Collinson, *Pollen Analysis*, 3rd Edition (Blackwell, Oxford, 1994).
43. P. Reimer, W. E. N. Austin, E. Bard, et al., "The IntCal20 Northern hemisphere radiocarbon age calibration curve (0–55 cal KBP)," Radiocarbon **62**, 725–757 (2020).
44. I. Renberg, M. L. Branvall, R. Bindler, and O. Emteryd, "Stable lead isotopes and lake sediments – a useful combination for the study of atmospheric lead pollution history," Sci. Total Environ. **292**, 45–54 (2002).

45. A. Rosentau, M. Muru, A. Kriiska, et al., "Stone Age settlement and Holocene shore displacement in the Narva-Luga Klint Bay area, eastern Gulf of Finland," Boreas **42**, 912–931 (2013).

46. D. Ryabchuk, A. Sergeev, V. Zhamoida, et al., "High-Resolution Geological Mapping Towards an Understanding of Post-Glacial Development and Holocene Sedimentation Processes in the Eastern Gulf of Finland: An EMODnet Geology Case Study," in *From Continental Shelf To Slope: Mapping the Oceanic Realm*, Ed. by K. Asch, H. Kitazato, and H. Vallius (Geological Society, London, 2020).

47. D. Ryabchuk, V. Zhamoida, A. Amantov, et al., "Development of the Coastal Systems of the Easternmost Gulf of Finland, and Their Links with Neolithic-Bronze and Iron Age Settlements," in *Geology and Archaeology: Submerged Landscapes of the Continental Shelf*, Ed. by J. Harff, G. Bailey, and F. Luth F (Geological Society, London, 2016).

48. D. V. Ryabchuk, A. Yu. Sergeev, D. V. Prishchepenko, et al., "Impact of climate change on sedimentation processes in the eastern Gulf of Finland during the middle to late Holocene," Boreas **50**, 381–403 (2021).

49. L. Sagnotti, "Demagnetization analysis in Excel (DAIE). An open source workbook in excel for viewing and analyzing demagnetization data from paleomagnetic discrete samples and u-channels," Ann. Geophysics **56**, D0114 (2013).

50. I. Snowball, L. Zillen, A. Ojala, et al., "FENNOSTACK and FENNORPIS: Varve dated Holocene paleomagnetic secular variation and relative paleointensity stacks from Fennoscandia," Earth Planet. Sci. Lett. **255**, 106–116 (2007).

51. G. Sohlenius, J. Sternbeck, E. Andren, et al., "Holocene history of the Baltic Sea as recorded in a sediment core from the Gotland Deep," Mar. Geol. **134**, 183–201 (1996).

52. M. Spiridonov, D. Ryabchuk, A. Kotilainen, et al., "The Quaternary Deposits of the Eastern Gulf of Finland," in *Holocene Sedimentary Environment and Sediment Geochemistry of the Eastern Gulf of Finland, Baltic Sea*, Ed. by H. Vallius, Geol. Surv. of Finland **45**, 5–17 (2007).

53. M. Spiridonov, A. Rybalko, V. Butylin, et al., "Modern Data, Facts and Views on the Geological Evolution of the Gulf of Finland," in *The Baltic Sea*, Ed. by B. Winterhalter, Geological Survey of Finland Special Paper **6**, 95–100 (1988).

54. S. Uscinowicz, *Geochemistry of Baltic Sea Surface Sediments* (Pol. Geol. Inst.-Nat. Res. Inst., Warsaw, 2011).

55. J. J. Virtasaalo, D. Ryabchuk, A. T. Kotilainen, et al., "Middle Holocene to present sedimentary environment in the easternmost Gulf of Finland (Baltic Sea) and the birth of the Neva River," Mar. Geol. **350**, 84–96 (2014).

56. J. J. Virtasalo, L. Lowemark, H. Papunen, et al., "Pyritic and baritic burrows and microbial filaments in postglacial Lacustrine clays in the northern Baltic Sea," J. Geol. Soc. **167**, 1185–1198 (2010).

57. L. Warden, M. Moros, T. Neumann, et al., "Climate induced human demographic and cultural change in Northern Europe during the mid-Holocene," Sci. Rep. **7**, 1–11 (2017).

58. B. Winterhalter, "Late-quaternary stratigraphy of Baltic Sea basins: a review," Bull. the Geolog. Soc. Finland **64** (1992).

59. L. Zillen, C. Lenz, and T. Jilbert, "Stable lead (Pb) isotopes and concentrations – a useful independent dating tool for Baltic sea sediments," Quat. Geochronology **8**, 41–45 (2012).